Level Spacing Statistics, Integrability and Many-Body Localization in Quantum Spin Chains

Leonardo Coscia[1*]

[1]Physics Department, University of Pisa

Abstract

The statistical properties of quantum spectra have been shown to be useful tools for identifying the integrability of quantum systems and the ergodicity of quantum many-body phases. In this work, we study, through numerical diagonalization, the level spacing statistics of two quantum spin chains: a quantum Ising chain in a transverse and longitudinal field, and a disordered Heisenberg XXZ chain. The former model is integrable in the absence of a longitudinal field, while the latter exhibits a transition from an ergodic to a many-body localized phase when increasing the strength of the disorder. By computing the level spacing distribution, we observe the transition from Poissonian to Wigner–Dyson statistics in the Ising model when introducing a longitudinal field, and the transition from Wigner–Dyson to Poissonian statistics in the Heisenberg XXZ model when increasing the disorder strength.

Introduction

The statistical properties of quantum spectra provide a framework for distinguishing between integrable and nonintegrable many-body systems [1]. In particular, the object of study is the distribution of spacings between energy levels. The intuition behind this approach is that integrable systems, characterized by a great number of conserved quantities, exhibit uncorrelated spectra belonging to different symmetry sectors. Energy levels belonging to different sectors, therefore, can cross each other freely when changing the system parameters. If one is to imagine studying a particular Hamiltonian as sampling an arbitrary point in the space of system parameters, it is easy to see that, in this case, level spacings arbitrarily close to zero should be expected. In contrast, when the symmetries of the system are broken, one expects to see avoided crossings, given that the energy levels can now interact. In this case, the probability of finding two levels arbitrarily close to each other is vanishingly small.

Beyond this intuitive picture, there are mathematical predictions as to the exact distribution of level spacings, which are due to the field of random matrix theory (RMT). It is important to note, though, that these are conjectures, even if extensively corroborated by numerical results. The basics of the theory are:

1. the Berry–Tabor conjecture [2], which states that the unfolded level spacings s of integrable systems are Poisson distributed
$$P(s) = \frac{1}{\langle s \rangle} e^{-s/\langle s \rangle}; \tag{1}$$
2. the Bohigas–Giannoni–Schmit conjecture [3], which asserts that the unfolded level spacings s of chaotic systems follow the statistics characteristic of different ensembles of random matrices, depending on the symmetries of the system. In particular, for systems with time-reversal symmetry, the unfolded level spacings are distributed according to the Wigner–Dyson distribution
$$P(s) = \frac{\pi s}{2\langle s \rangle^2} e^{-\frac{\pi s^2}{4\langle s \rangle^2}}, \tag{2}$$
derived from the Gaussian orthogonal ensemble (GOE).

In the first section of this work, we examine a periodic quantum Ising chain in a transverse field. This is, through a Jordan-Wigner transformation, mappable to a system of free fermions, and is therefore integrable. We then introduce a longitudinal field, which breaks the integrability of the model. By computing the level spacing statistics in the absence or presence of the longitudinal field, we observe the transition from Poissonian to Wigner–Dyson statistics.

The same statistical analysis can be used to study the phenomenon of disorder-induced [4] many-body localization (MBL). Similarly to energy levels in integrable systems not interacting due to symmetry, in a many-body localized phase the eigenstates of the system are localized in the Hilbert space of the system, and therefore do not interact with each other. This leads to level crossings and Poissonian level spacing

*Professor: Davide Rossini
Written: September 28, 2025, **Submitted:** October 10, 2025

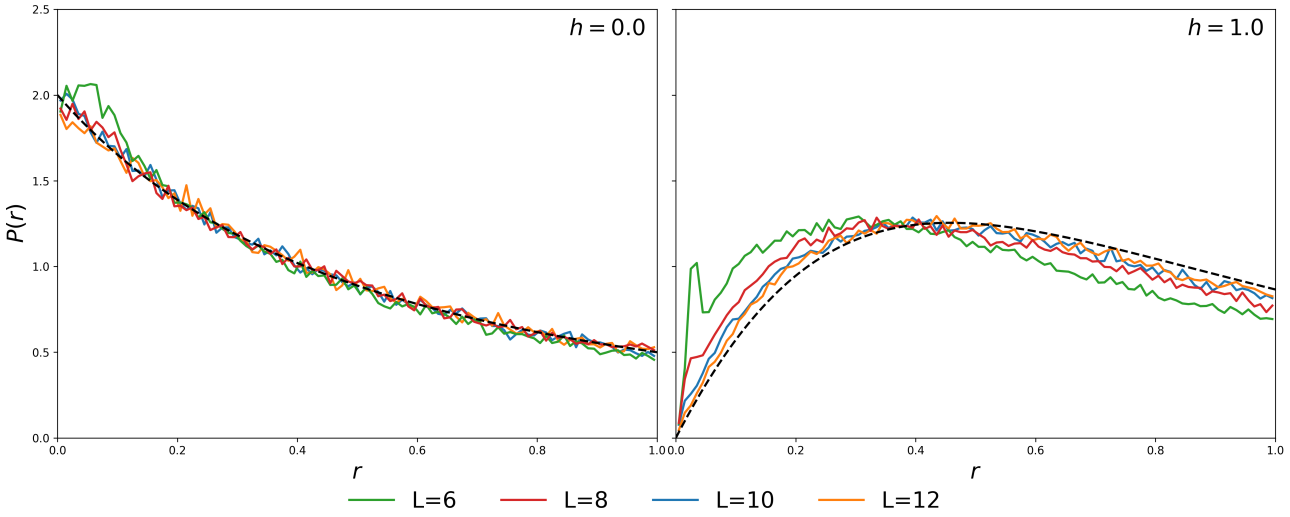

Figure 1: *Plot of the level spacing ratio distribution for Ising chains of size $L = 6, 8, 10, 12$, transverse field $g = 1.0$, and disorder strength $\delta g = 0.5$. In black, the predicted distributions of Eqs. 4 and 5 appropriate for $h = 0$ and $h = 1$, respectively. The distributions are averaged over 2^{18-L} disorder realizations.*

statistics [5]. In contrast, in the ergodic phase, the eigenstates are extended, and interact strongly, leading to avoided crossings and Wigner–Dyson statistics [5]. This is only a crude picture of the phenomenon; the statistical properties of MBL phases have not been proven in general, but numerical studies have extensively corroborated the expected behaviour.

In the second section of this work, we study a disordered Heisenberg XXZ chain, which is known to exhibit a transition from an ergodic to a many-body localized phase when increasing the strength of the disorder. We observe this transition by computing the level spacing statistics for different values of the disorder strength and of the anisotropy.

LSS of the Ising Model

Model Hamiltonian

The one-dimensional quantum Ising model in a transverse field is described by the Hamiltonian

$$\hat{H}_0 = -\sum_{i=1}^{L} \hat{\sigma}_i^x \hat{\sigma}_{i+1}^x - g \sum_{i=1}^{L} \hat{\sigma}_i^z,$$

where $\hat{\sigma}_i^{x,y,z}$ are the Pauli matrices acting on site i and $i+1$ is taken modulo L (periodic boundary conditions).

The model is integrable, and can be mapped to a system of free fermions through a Jordan–Wigner transformation:

$$\hat{a}_i = \Big(\prod_{j<i} \hat{\sigma}_j^z\Big) \frac{\hat{\sigma}_i^x - i\hat{\sigma}_i^y}{2},$$

$$\hat{H}_0 = -\sum_{i=1}^{L} \big(\hat{a}_i^\dagger \hat{a}_{i+1} + \hat{a}_{i+1}^\dagger \hat{a}_i + \hat{a}_i^\dagger \hat{a}_{i+1}^\dagger + \hat{a}_{i+1}\hat{a}_i\big) + \\ - g \sum_{i=1}^{L} \big(2\hat{a}_i^\dagger \hat{a}_i - 1\big).$$

The fermionic Hamiltonian is quadratic, and can be diagonalized exactly through a Bogoliubov transformation. This is still the case when the transverse field is made site-dependent, i.e. $g \to g_i$. The model is no longer integrable, however, when a longitudinal field is introduced:

$$\hat{H} = \hat{H}_0 - h \sum_{i=1}^{L} \hat{\sigma}_i^x.$$

The longitudinal field breaks the integrability of the model, and the Hamiltonian can no longer be mapped to a quadratic fermionic Hamiltonian:

$$\hat{\sigma}_i^x = \hat{a}_i^\dagger e^{-i\pi \sum_{j<i} \hat{a}_j^\dagger \hat{a}_j} + \hat{a}_i e^{+i\pi \sum_{j<i} \hat{a}_j^\dagger \hat{a}_j}.$$

In the interest of breaking all symmetries of the model, we choose a random transverse field, i.e. $g_i = g + \delta g_i$, where δg_i is a random number uniformly distributed in $[-\delta g, \delta g]$. This also lets us average over the disorder to enhance the statistics. The final Hamiltonian is therefore:

$$\hat{H} = -\sum_{i=1}^{L} \hat{\sigma}_i^x \hat{\sigma}_{i+1}^x - \sum_{i=1}^{L} g_i \hat{\sigma}_i^z - h \sum_{i=1}^{L} \hat{\sigma}_i^x. \qquad (3)$$

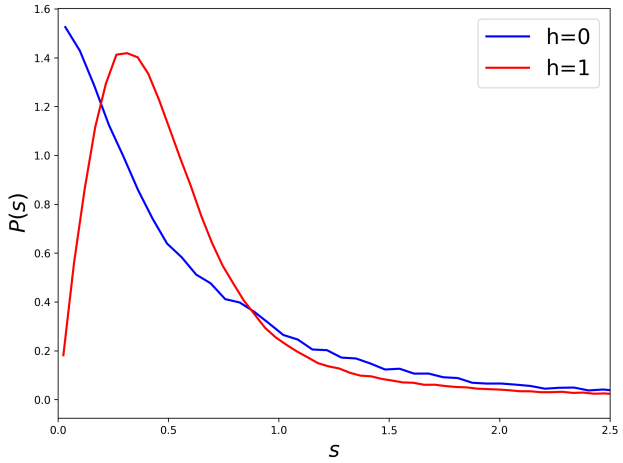

Figure 2: *Plot of the level spacing distribution for an Ising chain of size $L = 12$, transverse field $g = 1.0$, and disorder strength $\delta g = 0.5$. In blue, the case with no longitudinal field ($h = 0$), which is integrable and therefore is peaked at $s = 0$; in red, the case with a longitudinal field ($h = 1$), which is nonintegrable and therefore goes to zero linearly at the origin. The distributions are averaged over 64 disorder realizations.*

Numerical Analysis

The Hamiltonian (3) is written in the computational basis (eigenbasis of the $\hat{\sigma}_i^z$ operators) and is numerically diagonalized[1] for different values of the longitudinal field h and of the disorder strength δg. The level spacings are computed as $s_n = E_{n+1} - E_n$, where E_n are the eigenvalues of the Hamiltonian sorted in ascending order. The spacings are then normalized to their average value, i.e. $s_n \to s_n / \langle s \rangle$, where the average is taken over all level spacings and over all disorder realizations. The distribution of level spacings for all realizations is then computed by binning the normalized spacings.

These are the raw level spacings. To compare them to the theoretical predictions (1) and (2), we would need to perform an unfolding procedure [7], which consists in computing the cumulative distribution function $I(E)$ of each spectrum, fitting it with a smooth function $\tilde{I}(E)$ (usually polynomial), then defining the unfolded energies $\varepsilon_n = \tilde{I}(E_n)$. The unfolded spacings are computed and then the binning over realizations is performed.

This is a very involved procedure, but it is not the only way to analyze the level spacings. It is much easier to compute the ratio of consecutive level spacings [5], defined as

$$r_n = \frac{\min(s_n, s_{n+1})}{\max(s_n, s_{n+1})} \in [0, 1].$$

This quantity is dimensionless and confined to a fixed range, and is therefore easier to work with when comparing different systems. In the Poissonian case (1), the distribution of r is given by [8]

$$\begin{aligned} P_{\mathrm{p}}(r) &= \frac{2}{(1+r)^2} \\ \langle r \rangle_{\mathrm{p}} &= 2\ln(2) - 1 \simeq 0.3863. \end{aligned} \tag{4}$$

In the Wigner–Dyson case (2), the distribution of r is given by [8]

$$\begin{aligned} P_{\mathrm{w}}(r) &= \frac{27}{4} \frac{r + r^2}{(1 + r + r^2)^{5/2}}, \\ \langle r \rangle_{\mathrm{w}} &= 4 - 2\sqrt{3} \simeq 0.5359. \end{aligned} \tag{5}$$

In Fig. 2, we can see that in the absence of a longitudinal field ($h = 0$), the level spacing distribution has a peak at $s = 0$, while it goes to zero linearly in the presence of a longitudinal field ($h = 1$). The distributions are, qualitatively, what we expect, but they are not quantitatively compatible with the theoretical predictions (1) and (2). This is because the spectrum has not been unfolded.

In Fig. 1, we show the distributions of the ratios, in the presence or absence of a longitudinal field. The results for different system sizes are compared with the theoretical predictions of Eqs. 4 and 5. We can see that the compatibility with theory gets better with system size, and is, for the biggest size $L = 12$, very good.

In Fig. 3, we show the distributions of the ratios for different values of the transverse field g. The results are compatible with the theoretical predictions of Eqs. 4 and 5 for the smallest values of g, but deviate from them for larger values. This is due to the fact that, for large g, the transverse field term dominates the Hamiltonian, and the system becomes effectively integrable again. This has also been seen in [1].

MBL in Heisenberg XXZ Model

Model Hamiltonian

The one-dimensional Heisenberg XXZ model is described by the Hamiltonian

$$\hat{H}_0 = -\sum_{i=1}^{L} \left(\hat{\sigma}_i^x \hat{\sigma}_{i+1}^x + \hat{\sigma}_i^y \hat{\sigma}_{i+1}^y + \Delta \hat{\sigma}_i^z \hat{\sigma}_{i+1}^z \right),$$

where Δ is the anisotropy parameter and periodic boundary conditions are assumed.

The model is integrable, and can be solved exactly through the Bethe ansatz [9, 10]. We introduce disorder in the model by adding a random magnetic field in the z direction:

$$\hat{H} = \hat{H}_0 - \sum_{i=1}^{L} g_i \hat{\sigma}_i^z,$$

[1] Using the Eigen library for C++ [6].

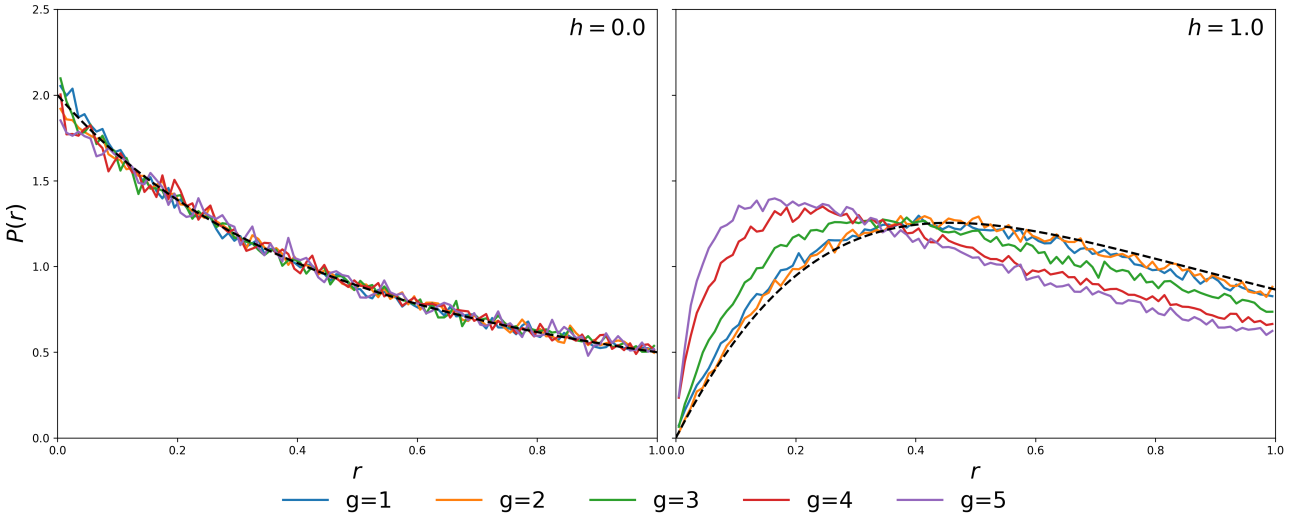

Figure 3: *Plot of the level spacing ratio distribution for an Ising chain of size* $L = 11$*, transverse fields* $g = 1.0, 2.0, 3.0, 4.0, 5.0$*, and disorder strength* $\delta g = 0.5$*. In black, the predicted distributions of Eqs. 4 and 5 appropriate for* $h = 0$ *and* $h = 1$*, respectively. The distributions are averaged over* 128 *disorder realizations.*

where g_i is a random number uniformly distributed in $[-g, g]$. The disordered Heisenberg XXZ model is known to exhibit a transition from an ergodic to a many-body localized phase when increasing the strength of the disorder g, for any value of the anisotropy Δ.

The final Hamiltonian is therefore:

$$\hat{H} = -\sum_{i=1}^{L} \left(2\hat{\sigma}_i^+ \hat{\sigma}_{i+1}^- + 2\hat{\sigma}_i^- \hat{\sigma}_{i+1}^+ + \Delta \hat{\sigma}_i^z \hat{\sigma}_{i+1}^z\right) + - \sum_{i=1}^{L} g_i \hat{\sigma}_i^z. \tag{6}$$

Measures of Localization

Following the example of [11], we consider three measures of localization: the level spacing statistics (LSS), the Kullback-Leibler divergence (KLD) of adjacent levels, and the bipartite entanglement entropy (BEE) of eigenstates.

LSS. As mentioned in the introduction, the level spacings are expected to follow Wigner–Dyson statistics in the ergodic phase and Poissonian statistics in the MBL phase. Therefore, by computing the level spacing statistics for different values of the disorder strength g and of the anisotropy Δ, we can observe the transition from the ergodic to the MBL phase.

KLD. The Kullback-Leibler divergence is a measure of distinguishability between quantum states. Given two pure states $|\psi\rangle$ and $|\phi\rangle$, the KLD is defined as

$$D_{\mathrm{KL}}(\psi|\phi) = \sum_i |\langle i|\psi\rangle|^2 \ln \frac{|\langle i|\psi\rangle|^2}{|\langle i|\phi\rangle|^2},$$

where $|i\rangle$ is a complete orthonormal basis (in our case, the computational basis). The KLD is non-negative, and is zero if and only if the two states are identical. In the context of MBL, we consider the KLD between adjacent eigenstates of the Hamiltonian, i.e. $|\psi_n\rangle$ and $|\psi_{n+1}\rangle$. In the ergodic phase, the eigenstates are extended and therefore have a significant overlap, leading to a small KLD. In the MBL phase, the eigenstates are localized and therefore have a small overlap, leading to a large KLD. Therefore, by computing the average KLD between adjacent eigenstates for different values of the disorder strength g and of the anisotropy Δ, we can observe the transition from the ergodic to the MBL phase.

BEE. The bipartite entanglement entropy is a measure of entanglement between two subsystems of a quantum system. Given a pure state $|\psi\rangle$ of a bipartite system $A \cup B$, the BEE is defined as

$$S_A = -\mathrm{Tr}_A(\hat{\rho}_A \ln \hat{\rho}_A),$$

where $\hat{\rho}_A = \mathrm{Tr}_B(|\psi\rangle\langle\psi|)$ is the reduced density matrix of subsystem A. When studying MBL, we consider the BEE of the eigenstates of the Hamiltonian, bipartitioning the system in two equal halves. In the ergodic phase, the eigenstates are extended and therefore have a large BEE, scaling with the volume of the subsystem (volume law). In the MBL phase, the eigenstates are localized and therefore have a small BEE, scaling with the area of the partitioning surface (area law). Therefore, by computing the average BEE of the eigenstates for different values of the disorder strength g and of the anisotropy Δ, we can observe the transition from the ergodic to the MBL phase.

Numerical Analysis

The Hamiltonian (6) is written in the computational basis (eigenbasis of the $\hat{\sigma}_i^z$ operators) and is numerically diagonalized for different values of the disorder strength g and of the anisotropy Δ. Again following [11], we restrict our analysis to the zero magnetization sector and limit ourselves to finding the closest 50 eigenvalues to the center of the spectrum, given that the point at which the MBL transition occurs is energy dependent, as shown in [11]. To do this we utilize Krylov space methods[2], applied to the shifted-inverted Hamiltonian $(H - E_{1/2})^{-1}$, where $E_{1/2}$ is the center of the spectrum, computed through a preliminary diagonalization to obtain the extremal eigenvalues. The shift-inverted method allows us to find the eigenvalues closest to $E_{1/2}$, which are the largest in magnitude for the shifted-inverted Hamiltonian.

For each partial spectrum we obtain, one for each realization, we compute the level spacings, the KLD between adjacent eigenstates, and the BEE of each eigenstate. The results are then averaged over all realizations, with a caveat [11]:

- for the KLD and BEE, all eigenstates in each realization are equivalent, therefore the average and the standard deviation are computed over all eigenstates of all realizations;
- for the LSS, the relevant quantity we want to compute is $\langle r \rangle$, which is a single number for each realization. Therefore, we first compute $\langle r \rangle$ for each realization, and then average over all realizations.

The difference is subtle, but important, as it changes how we compute the error bars:

$$\sigma_r^2 = \frac{[\langle r \rangle^2] - [\langle r \rangle]^2}{R - 1},$$
$$\sigma_{D_{\mathrm{KL}}}^2 = \frac{[\langle D_{\mathrm{KL}}^2 \rangle] - [\langle D_{\mathrm{KL}} \rangle]^2}{(N-1)R - 1},$$
$$\sigma_{S_A}^2 = \frac{[\langle {S_A}^2 \rangle] - [\langle S_A \rangle]^2}{NR - 1},$$

where N is the number of eigenstates computed, R is the number of realizations and the average over eigenstates in a realization and the average over realizations are denoted by $\langle\,\rangle$ and $[\,]$ respectively.

The results, for $L = 14$, are shown in Figs. 4, 5 and 6. For small disorder strengths (very roughly, for $g \lesssim 3$), the system is in the ergodic phase: r is compatible with the Wigner-Dyson distribution of Eq. 5, the KLD is small and independent of g, and the BEE is large and independent of g. As the disorder strength increases, the system undergoes a transition to the MBL phase, characterized by a value of r compatible with the Poisson distribution of Eq. 4, large (and growing) KLD, and small (and decreasing) BEE.

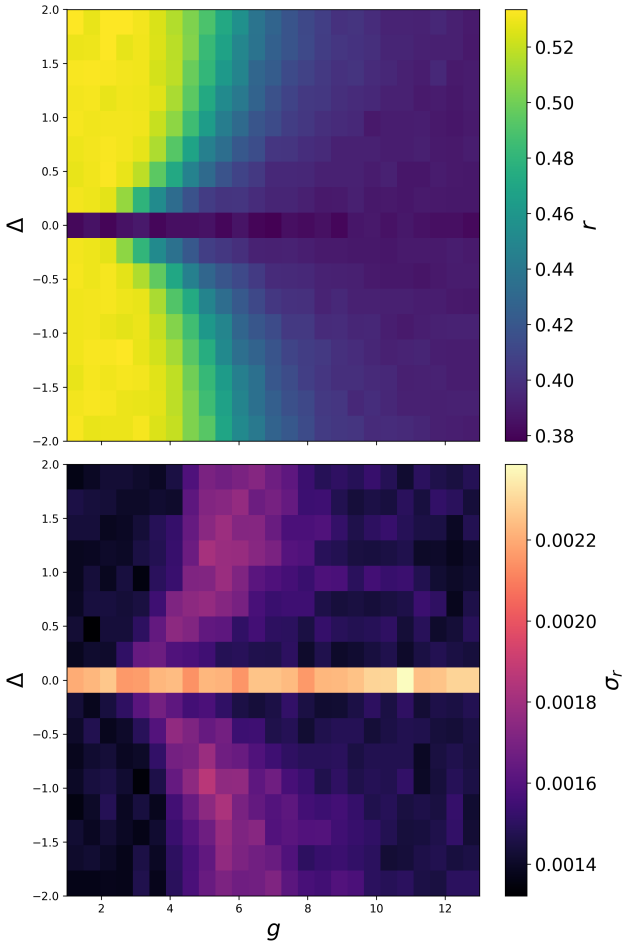

Figure 4: *At the top, plot of the average ratio r (at the center of the spectrum for $L = 14$) as a function of disorder strength g and anisotropy Δ in a Heisenberg XXZ chain. At the bottom, plot of the standard deviation σ_r. At high disorder strengths the system is in the MBL phase, with a value of r compatible with Eq. 4, while at low disorder strengths the system is ergodic, with a value of r compatible Eq. 5. We also see that an increase in uncertainty marks the transition. Larger values of Δ lead to a transition at larger disorder strengths. At $\Delta = 0$, the system is always at r_{p}.*

The transition point depends on the anisotropy Δ, with larger values of Δ leading to a transition at larger disorder strengths. We also see that the transition edge is marked by an increase in fluctuations for r and for S_A, as noted in [11].

At $\Delta = 0$, we see that the system does not follow the expected behaviour, as r remains fixed at r_{p} and both entropy and divergence do not reach a plateau. This is because, for this value of anisotropy, the system is an XY Heisenberg model in transverse field, which is integrable. No amount of disorder can alter the Poissonian nature of the level spacings. We also

[2] As implemented in the Spectra library for C++ [12].

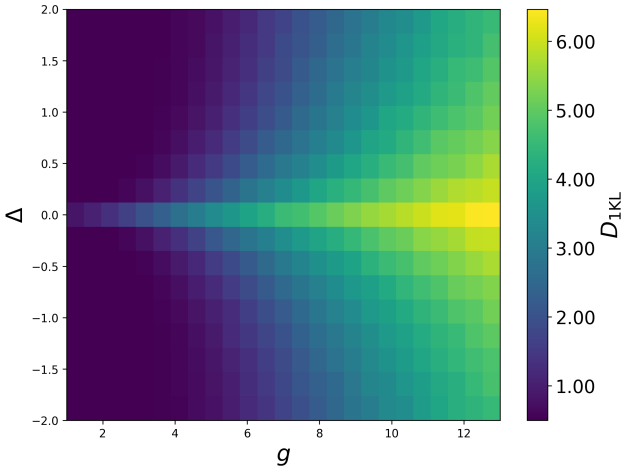

Figure 5: *Plot of the average KLD (at the center of the spectrum for $L = 14$) as a function of disorder strength g and anisotropy Δ in a Heisenberg XXZ chain. At low disorder the system is ergodic, with the KLD being small and independent of disorder. At $\Delta = 0$ and at high disorder, the KLD grows with disorder. Larger values of Δ lead to a transition at larger disorder strengths. No interesting behaviour is seen in the fluctuations.*

see that, the closer the system is to integrability, the bigger the MBL (Poissonian) phase is.

In Fig. 7, we show cross-sections of the previous plots for $\Delta = 0$ and $\Delta = 1$ respectively, for different system sizes. The error bars are computed as explained above. We can see that, for $\Delta = 0$, the system is always at r_{p}, while both KLD and BEE do not reach a plateau. For $\Delta = 1$, we see a clear transition from the ergodic to the MBL phase. The sharpness of the transition improves with system size, as does the agreement with Eqs. 4 and 5.

We can also see that BEE increases linearly with system size in the ergodic phase: this is a signature of the volume law scaling of entanglement entropy in ergodic systems. Similarly, KLD increases linearly with system size in the MBL phase: as the size increases, the localized eigenstates become more and more "distant" in Fock space, therefore the KLD increases. We have not found a theoretical prediction for the scaling of KLD with system size in the MBL phase, and it is difficult to affirm that it is linear, given the small range of system sizes we can access. Nonetheless, the same behaviour is seen in [11].

Code Implementation

All of the code used to perform the numerical analysis above is freely available at https://github.com/coscialeo/num_meth.git. The code is written in C++, and uses the Eigen [6] and Spectra [12] libraries for linear algebra and eigenvalue problems. The code is parallelized using OpenMP [13].

Python was used for data analysis and plotting,

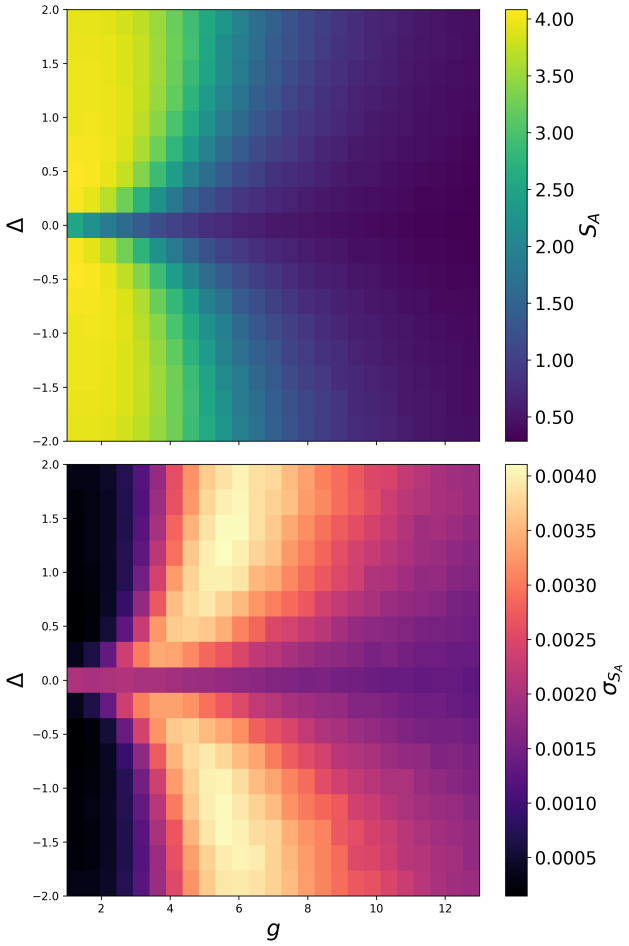

Figure 6: *At the top, plot of the average BEE (at the center of the spectrum for $L = 14$) as a function of disorder strength g and anisotropy Δ in a Heisenberg XXZ chain. At the bottom, plot of the standard deviation σ_{S_A}. At high disorder strengths and at $\Delta = 0$, the system is in the MBL phase, with the entropy decreasing with disorder, while at low disorder strengths the system is ergodic, with the BEE remaining constant and high. We also see that an increase in uncertainty marks the transition. Larger values of Δ lead to a transition at larger disorder strengths.*

using the NumPy and Matplotlib libraries. These scripts are not included in the repository.

References

[1] J. Karthik, A. Sharma, and A. Lakshminarayan. "Entanglement, avoided crossings, and quantum chaos in an Ising model with a tilted magnetic field". In: *Phys. Rev. A* 75 (2 Feb. 2007), p. 022304. DOI: 10.1103/PhysRevA.75.022304.

[2] M. V. Berry and M. Tabor. "Level clustering in the regular spectrum". In: *Proceedings of the Royal Society of London. A. Mathematical and Physical Sciences* 356.1686 (1977), pp. 375–394. DOI: 10.1098/rspa.1977.0140.

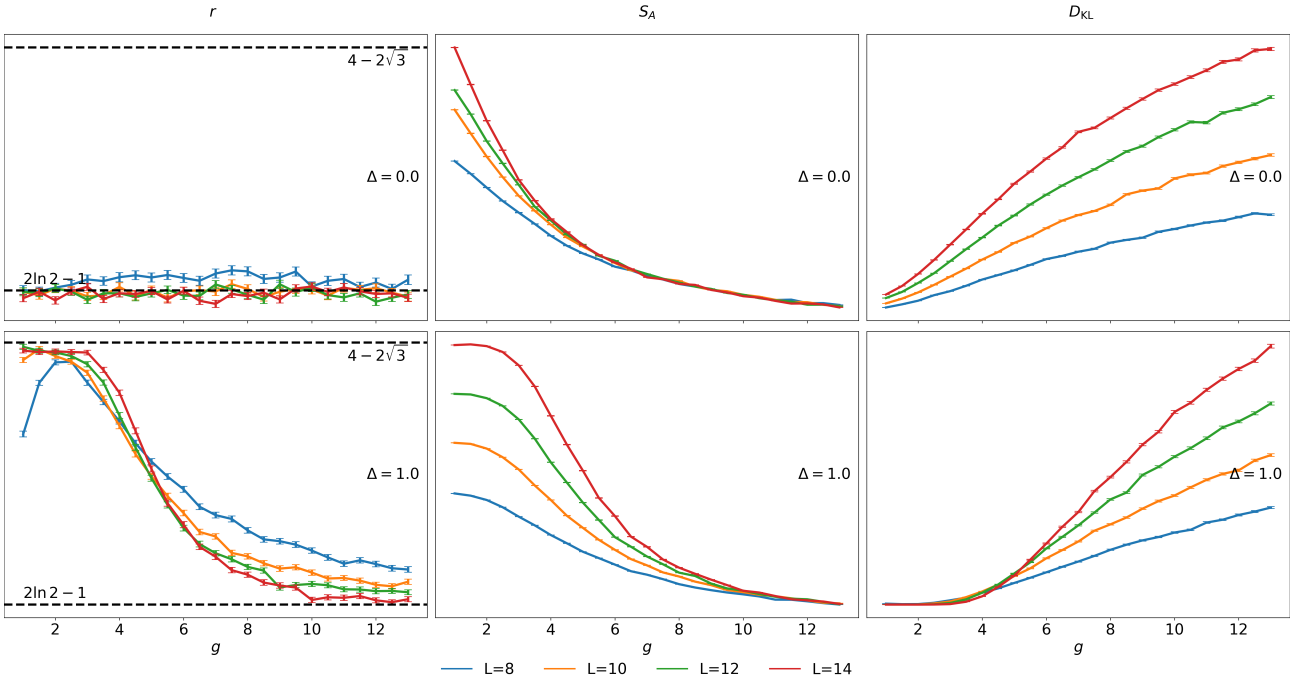

Figure 7: *Plots of the average ratio r (left), BEE (middle) and KLD (right) as a function of disorder strength g for* $\Delta = 0$ *(top) and* $\Delta = 1$ *(bottom), for Heisenberg XXZ chains of different lengths. The dashed lines are the theoretical predictions for the Poissonian and Wigner-Dyson distributions. The error bars are computed as explained in the text. For* $\Delta = 0$*, the system is always at* r_p*, while both KLD and BEE do not reach a plateau. For* $\Delta = 1$*, we see a clear transition from the ergodic to the MBL phase, with r going from* r_w *to* r_p*, KLD increasing with disorder and BEE decreasing with disorder. The sharpness of the transition improves with system size, as does the agreement with Eqs. 4 and 5. We can also see that BEE increases linearly with system size in the ergodic phase, while KLD does the same, in the MBL phase.*

[3] O. Bohigas, M. J. Giannoni, and C. Schmit. "Characterization of Chaotic Quantum Spectra and Universality of Level Fluctuation Laws". In: *Phys. Rev. Lett.* 52 (1 Jan. 1984), pp. 1–4. DOI: 10.1103/PhysRevLett.52.1.

[4] D.M. Basko, I.L. Aleiner, and B.L. Altshuler. "Metal–insulator transition in a weakly interacting many-electron system with localized single-particle states". In: *Annals of Physics* 321.5 (May 2006), pp. 1126–1205. ISSN: 0003-4916. DOI: 10.1016/j.aop.2005.11.014.

[5] V. Oganesyan and D. A. Huse. "Localization of interacting fermions at high temperature". In: *Phys. Rev. B* 75 (15 Apr. 2007), p. 155111. DOI: 10.1103/PhysRevB.75.155111.

[6] G. Guennebaud and B. Jacob. *Eigen v3*. http://eigen.tuxfamily.org. 2010.

[7] I. O. Morales, E. Landa, et al. "Improved unfolding by detrending of statistical fluctuations in quantum spectra". In: *Phys. Rev. E* 84 (1 July 2011), p. 016203. DOI: 10.1103/PhysRevE.84.016203.

[8] Y. Y. Atas, E. Bogomolny, et al. "Distribution of the Ratio of Consecutive Level Spacings in Random Matrix Ensembles". In: *Phys. Rev. Lett.* 110 (8 Feb. 2013), p. 084101. DOI: 10.1103/PhysRevLett.110.084101.

[9] C. N. Yang and C. P. Yang. "One-Dimensional Chain of Anisotropic Spin-Spin Interactions. I. Proof of Bethe's Hypothesis for Ground State in a Finite System". In: *Phys. Rev.* 150 (1 Oct. 1966), pp. 321–327. DOI: 10.1103/PhysRev.150.321.

[10] C. N. Yang and C. P. Yang. "One-Dimensional Chain of Anisotropic Spin-Spin Interactions. II. Properties of the Ground-State Energy Per Lattice Site for an Infinite System". In: *Phys. Rev.* 150 (1 Oct. 1966), pp. 327–339. DOI: 10.1103/PhysRev.150.327.

[11] D. J. Luitz, N. Laflorencie, and F. Alet. "Many-body localization edge in the random-field Heisenberg chain". In: *Phys. Rev. B* 91 (8 Feb. 2015), p. 081103. DOI: 10.1103/PhysRevB.91.081103.

[12] Y. Qiu, G. Guennebaud, and J. Niesen. *Spectra: C++ library for large scale eigenvalue problems*. https://spectralib.org. 2015.

[13] L. Dagum and R. Menon. "OpenMP: An Industry-Standard API for Shared-Memory Programming". In: *IEEE Comput. Sci. Eng.* 5.1 (Jan. 1998), pp. 46–55. ISSN: 1070-9924. DOI: 10.1109/99.660313.